SCIENTIFIC REPORTS

OPEN

SUBJECT AREAS:
ENVIRONMENTAL MICROBIOLOGY
BACTERIAL TECHNIQUES AND APPLICATIONS

Received
1 October 2014

Accepted
29 December 2014

Published
27 January 2015

Correspondence and requests for materials should be addressed to X.S. (xihuishen@nwsuaf.edu.cn)

* These authors contributed equally to this work.

Functional characterization of a vanillin dehydrogenase in *Corynebacterium glutamicum*

Wei Ding[1]*, Meiru Si[1,2]*, Weipeng Zhang[1], Yaoling Zhang[1], Can Chen[1,2], Lei Zhang[1,2], Zhiqiang Lu[3], Shaolin Chen[2] & Xihui Shen[1,2]

[1]State Key Laboratory of Crop Stress Biology for Arid Areas and College of Life Sciences, Northwest A&F University, Yangling, Shaanxi 712100, PR China, [2]Biomass Energy Center for Arid and Semi-Arid Lands, Northwest A&F University, Yangling, Shaanxi 712100, PR China, [3]College of Plant Protection, Northwest A&F University, Yangling, Shaanxi 712100, PR China.

Vanillin dehydrogenase (VDH) is a crucial enzyme involved in the degradation of lignin-derived aromatic compounds. Herein, the VDH from *Corynebacterium glutamicum* was characterized. The relative molecular mass (Mr) determined by SDS-PAGE was ~51 kDa, whereas the apparent native Mr values revealed by gel filtration chromatography were 49.5, 92.3, 159.0 and 199.2 kDa, indicating the presence of dimeric, trimeric and tetrameric forms. Moreover, the enzyme showed its highest level of activity toward vanillin at pH 7.0 and 30°C, and interestingly, it could utilize NAD^+ and $NADP^+$ as coenzymes with similar efficiency and showed no obvious difference toward NAD^+ and $NADP^+$. In addition to vanillin, this enzyme exhibited catalytic activity toward a broad range of substrates, including *p*-hydroxybenzaldehyde, 3,4-dihydroxybenzaldehyde, *o*-phthaldialdehyde, cinnamaldehyde, syringaldehyde and benzaldehyde. Conserved catalytic residues or putative cofactor interactive sites were identified based on sequence alignment and comparison with previous studies, and the function of selected residues were verified by site-directed mutagenesis analysis. Finally, the *vdh* deletion mutant partially lost its ability to grow on vanillin, indicating the presence of alternative VDH(s) in *Corynebacterium glutamicum*. Taken together, this study contributes to understanding the VDH diversity from bacteria and the aromatic metabolism pathways in *C. glutamicum*.

Corynebacterium glutamicum, a fast growing Gram-positive soil bacterium, is one of the most important microorganisms in industrial biotechnology. Since its discovery, *C. glutamicum* has been widely used for industrial production of amino acids, vitamins, nucleotides and various other bio-based chemicals[1]. As a soil bacterium, recent studies have demonstrated that *C. glutamicum* is able to utilize a large variety of lignin derived aromatic compounds (e.g. vanillin, ferulate, *p*-coumarate, cinnamate, etc.) for growth[2,3]. The outstanding capability of *C. glutamicum* in assimilation of aromatic compounds provides it with a distinct advantage in using lignocellulosic hydrolysates as sustainable and inexpensive feedstocks in industrial fermentation, thanks to its capability to detoxify and assimilate great amounts of lignin derived aromatic inhibitors in lignocellulosic hydrolysates as an alternative source to sugars for carbon and energy.

The main lignin-derived aromatic inhibitors in lignocellulosic hydrolysates are ferulate, vanillin, *p*-coumarate, 4-hydroxybenzoic acid (4-HBA), and vanillic acid, and most of which can be assimilated into TCA cycle intermediates by *C. glutamicum*[3–5]. Catabolism of ferulate follows a CoA-dependent non-β-oxidative pathway that contains feruloyl-CoA synthetase (Fcs) and enoyl-CoA hydratase/aldolase (Ech), yielding vanillin[6]. Vanillin is further converted into protocatechuate catalyzed by an aldehyde dehydrogenase (Vdh) and a demethylase (VanAB)[7,8]. Although some peripheral pathways converting various phenylpropanoids (such as vanillin, vanillate, caffeate, *p*-coumarate, and cinnamate) to protocatechuate have been suggested in *C. glutamicum*, and the genes *van*AB encoding vanillate demethylase that catalyzes the conversion of vanillate to protocatechuate have been functionally identified[3,6], the upstream vanillin dehydrogenase gene (*vdh*) has not been experimentally investigated.

The vanillin dehydrogenase is a critical enzyme for the degradation of lignin derived phenylpropanoids (such as vanillin, vanillate, caffeate, *p*-coumarate, and cinnamate) and studies on vanillin dehydrogenase gene (*vdh*) in Gram-negtive bacteria have been well documented. For instance, *vdh* has been characterized in *Pseudomonas fluorescens*[9], *Pseudomonas putida*[10,11], *Pseudomonas* sp. strain HR199[12], and *Sphingomonas paucimobilis* SYK-

6[13,14]. When the *vdh* gene was deleted in *Pseudomonas fluorescens*, it completely lost the ability to utilize ferulic acid, vanillin, *p*-coumarate as carbon source but not 4-hydroxybenzaldehyde[9]. In addition, experimental results have confirmed that the *vdh* gene is associated with the degradation of vanillin, benzaldehyde, *p*-hydroxybenzaldehyde, protocatechualdehyde in *S. paucimobilis* SYK-6[13,14]. However, studies focusing on the vanillin dehydrogenase in Gram-positive bacteria were rare. This study indentified the gene coding for putative vanillin dehydrogenase in *C. glutamicum* and investigated the enzyme activity, substrate specificity and roles in catabolism of aromatic compounds in *C. glutamicum*, thus contributing to a deeper understanding of the aromatic metabolism pathways in *C. glutamicum*.

Results

Indentification of *vdh* gene from *C. glutamicum* genome and phylogenetic analysis. Based on BLAST Search and genome sequence analysis, the gene coding for a putative vanillin dehydrogenase (*ncgl2578*, named as $vdh_{ATCC13032}$ in this study) was identified, which composed of 1,455 bp and encoded a protein of 484 amino acids with a theoretical molecular mass of 51.5 kDa. The $vdh_{ATCC13032}$ shares 35%, 41% and 59% amino acid sequence identity with the *vdh* genes from *Pseudomonas aeruginosa* DK2, *Rhodococcus jostii* RHA1 and *Pseudomonas fluorescens*, respectively. To further assess the phylogenetic relationship between $vdh_{ATCC13032}$ and *vdh* genes from other bacteria, a multiple-sequence alignment was conducted using ClustalX 1.83 (Fig. 1). The results showed that the $vdh_{ATCC13032}$ from *C. glutamicum* forms an independent cluster on the phylogenetic tree and exhibits clear evolutionary distance with already verified *vdh* genes from other bacteria. These results suggested that *vdh* from *C. glutamicum* may therefore represent a new vanillin dehydrogenase branch and the $vdh_{ATCC13032}$ represents the first vanillin dehydrogenase characterized in detail within this gene family.

Functional characterization of gene $vdh_{ATCC13032}$ *in vivo*. To further characterize the vanillin dehydrogenase activity of $VDH_{ATCC13032}$, a mutant strain ($\Delta vdh_{ATCC13032}$) was obtained by homologous recombination based gene knock-out. Growth analyses of wild type strain and $\Delta vdh_{ATCC13032}$ were conducted in liquid media at 30°C, using different substrates such as vanillin (8 mM), *p*-hydroxybenzaldehyde (8 mM), 3,4-dihydroxybenzaldehyde (5 mM), 3-hydroxybenzaldehyde (5 mM), ferulic acid (3 mM), caffeic acid (3 mM), *p*-cresol (5 mM), cinnamyl aldehyde (5 mM) and syringaldehyde (2.5 mM)) as the sole carbon and energy source. Compared to the wild type, the $\Delta vdh_{ATCC13032}$ mutant showed remarkably reduced ability to grow with the above mentioned aromatic compounds (Fig. 2). When complemented with plasmid pXMJ19-$vdh_{ATCC13032}$, the growth ability of the mutant strain could be restored close to that of the wild type (Fig. 2). However, the wild type, the $\Delta vdh_{ATCC13032}$ mutant and the complementary strain showed no difference when grown in *p*-cresol, cinnamyl aldehyde and syringaldehyde (data not shown).

Heterologous expression and molecular mass (Mr) estimation of $VDH_{ATCC13032}$. To further study the biochemical function of $VDH_{ATCC13032}$, the gene was PCR-amplified and heterologously expressed in *E. coli*. The recombinant strain carrying pET28a-$vdh_{ATCC13032}$ showed vanillin dehydrogenase activity, and the purified recombinant VDH was estimated to have a relative Mr of about 51.1 kDa, as determined by sodium dodecyl sulfate polyacrylamide gel electrophoresis (SDS-PAGE) (Fig. 3A), consistent with the predicted Mr value. However, gel filtration chromatography analysis showed four peaks corresponding to molecular mass of 49.5, 92.3, 159.0 and 199.2 kDa, respectively, indicating the native $VDH_{ATCC13032}$ existing as tetramers, trimers and dimers (Fig. 3B). The existence of $VDH_{ATCC13032}$ in tetramer, trimer and dimer was also confirmed by native PAGE analysis (Fig. 3C).

Biochemical properties of $VDH_{ATCC13032}$. Purified enzyme preparations of $VDH_{ATCC13032}$ were found to be stable and could be stored at 4°C for 2 weeks without significant loss of activity. The influence of pH and temperature on the activity of $VDH_{ATCC13032}$ was investigated (Fig. 4). The highest activity was demonstrated to be at 30°C in accordance with the temperature of physiological habitat of *C. glutamicum* whereas the optimum pH observed for reaction was pH 7.0 (in 100 mM potassium phosphate buffer). Several aldehydes were selected as the potential substrates to test the substrate specificity and

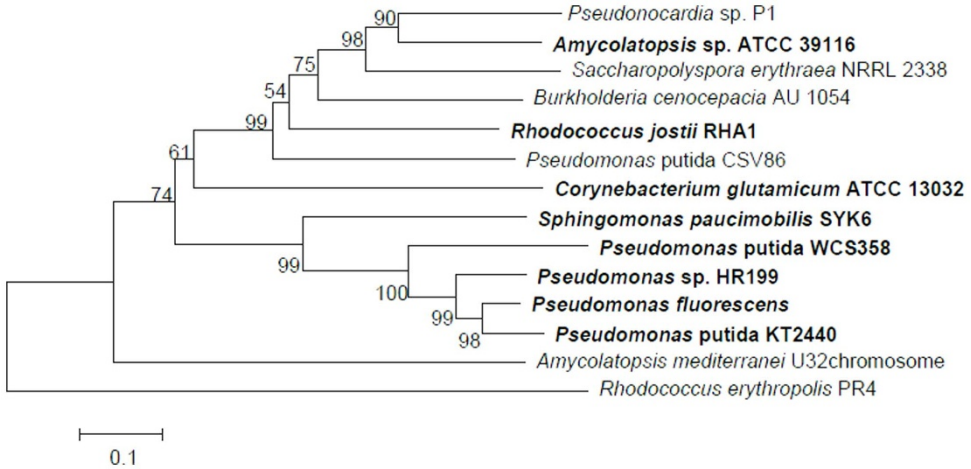

Figure 1 | Rooted neihbor-joining tree constructed from the amino acid sequence of 14 vanillin dehydrogenases. Boot strap confidence limits (expressed as percentage) are shown at nodes. Multiple-sequence alignment was done by using ClustalX 1.83 based on the amino acid sequences of the following enzymes: putative VDH of *C. glutamicum* ATCC13032 (NP_601867.1), benzaldehyde dehydrogenase of *Rhodococcus erythropolis* PR4[38,39], VDH of *Rhodococcus jostii* RHA1[40], VDH of *Sphingomonas paucimobilis* SYK-6[13,14], benzaldehyde dehydrogenase of *Pseudomonas putida* CSV86[11,41], VDH of *Pseudomonas putida* WCS358[42], VDH of *Pseudomonas putida* KT2440[10,43], VDH of *Pseudomonas* sp. HR199[24], VDH of *Amycolatopsis* sp. ATCC 39116[21], VDH of *Pseudomonas fluorescens*[32,44], aldehyde dehydrogenase (NAD^+) of *Pseudonocardia* sp. P1(ZP_08121488.1), benzaldehyde dehydrogenase (NAD^+) of *Saccharopolyspora erythraea* NRRL 2338(YP_001105347.1), benzaldehyde dehydrogenase (NAD^+) of *Burkholderia cenocepacia* AU 1054(YP_621190.1), and aldehyde dehydrogenase of *Amycolatopsis mediterranei* U32 (AMED_0881). Calculations were performed by using the neighbor-joining method. Enzymes with verified vanillin dehydrogenase activity are shown in boldface type.

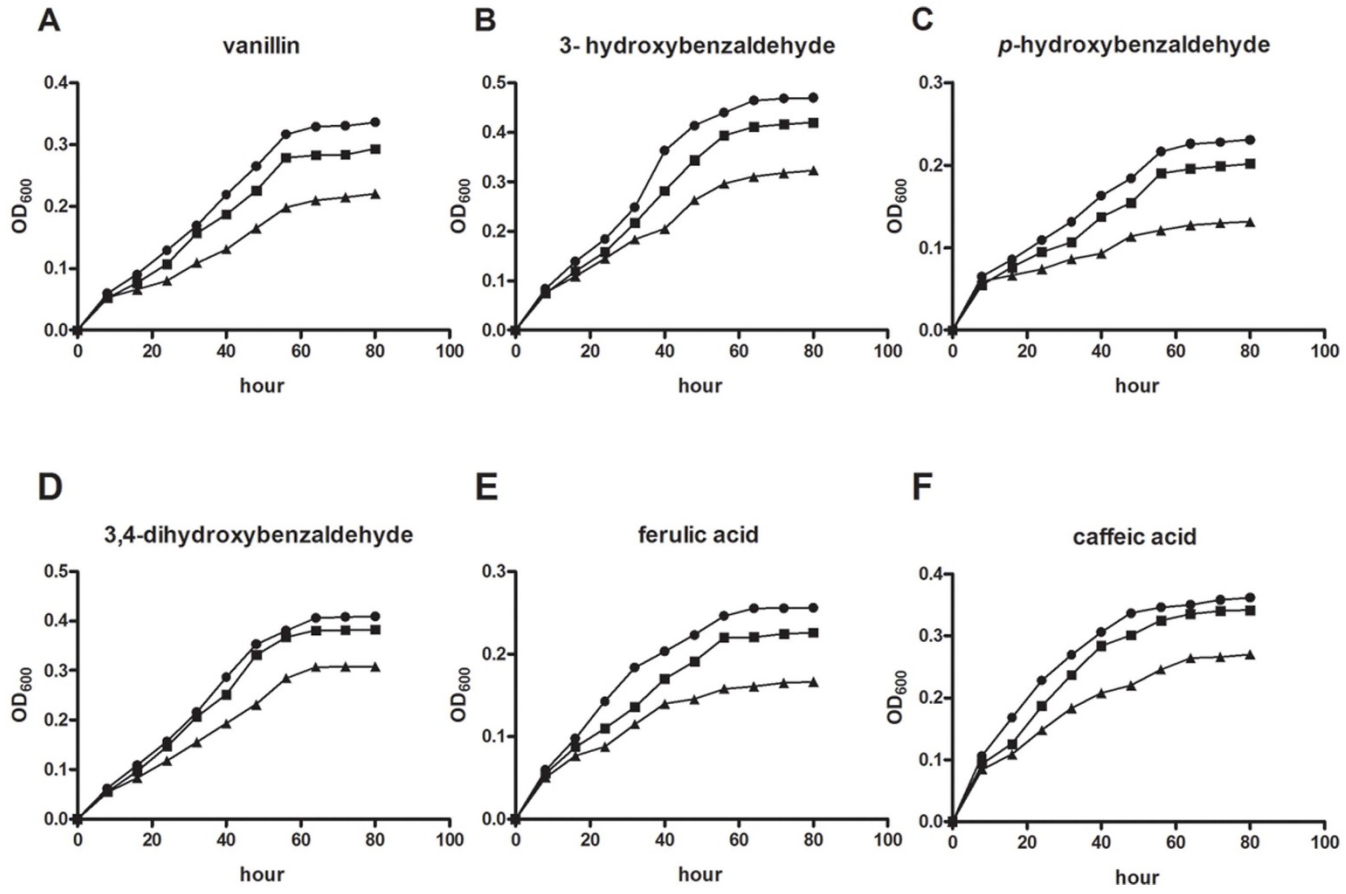

Figure 2 | **Phenotypic characterization of *Δvdh* and the complemented strain *Δvdh*(pXMJ19-*vdh*) grown on mineral salts medium containing 8 mM vanillin (A), 5 mM 3-hydroxybenzaldehyde (B), 8 mM *p*-hydroxy benzaldehyde (C), 5 mM 3,4-dihydroxybenzaldehyde (D), 3 mM ferulic acid (E) and caffeic acid (F), respectively. ⊸WT(pXMJ19), ⊸*Δvdh*(pXMJ19), ⊸*Δvdh*(pXMJ19-*vdh*).**

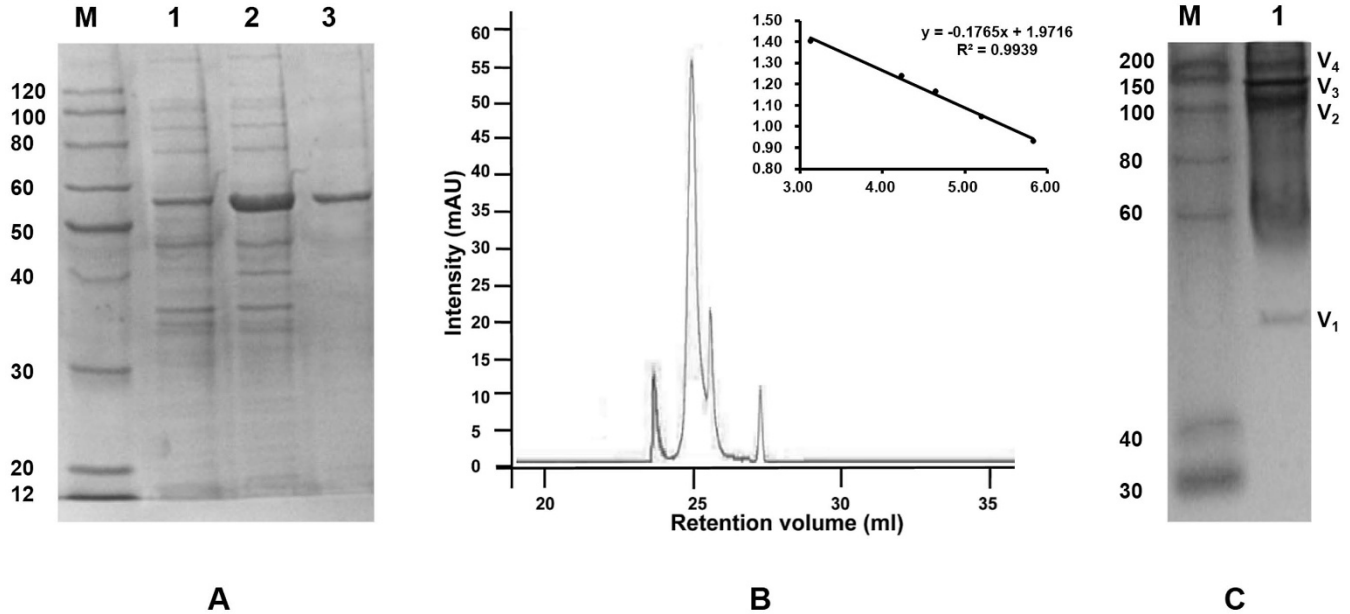

Figure 3 | **Molecular mass determination of the purified $VDH_{ATCC13032}$.** (A) SDS-PAGE analysis of $VDH_{ATCC13032}$. M: protein marker. Lane 1: cell extracts of *E. coli*/pET28a-*ncg12578* (not induced); lane 2: cell extracts of *E. coli*/pET28a-*ncg12578* (induced); Lanes 3: purified $VDH_{ATCC13032}$ after Ni-NTA affinity chromatography. (B) Gel filtration analysis of purified VDH_{ATCC}13032. Molecular weight standards from large to small weight: Thyroglobulin (bovine)(670 kDa), γ-globulin (bovine)(158 kDa), Ovalbumin (chicken)(44 kDa), Myoglobin (horse)(17 kDa) and Vitamin B_{12}(1.35 kDa). The molecular weight of purified $VDH_{ATCC13032}$ was estimated using the above molecular weight standards. (C) Typical appearance of native-PAGE obtained by loading 40 μg of purified $VDH_{ATCC13032}$. The position of the monomer (V_1), dimer (V_2), trimer (V_3) and tetramer (V_4) of VDH are indicated.

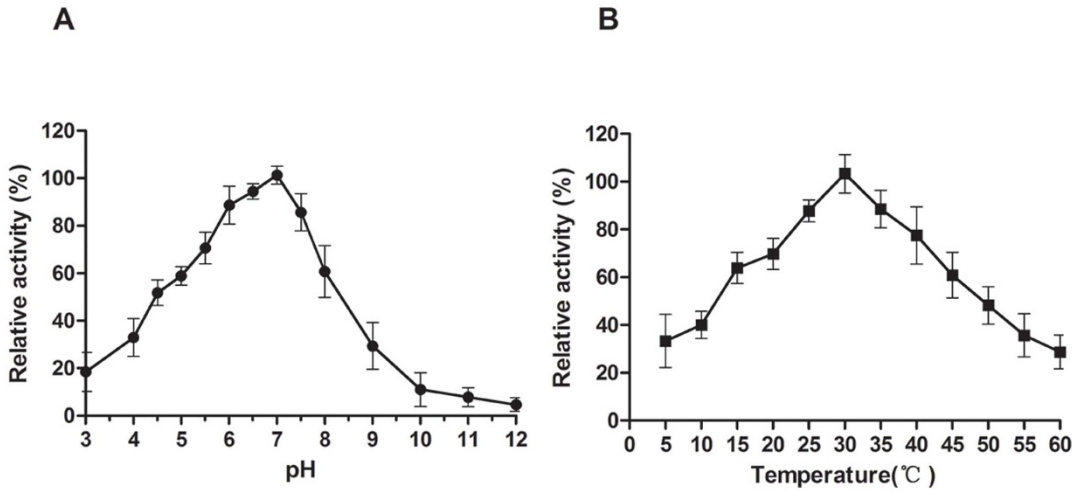

Figure 4 | pH (A) and temperature (B) optimum of purified $VDH_{ATCC13032}$. (A) The optimum pH was measured at room temperature in buffers with different pHs using vanillin as the substrate. The optimal pH was determined in various pHs of 100 mM buffer as follows: glycine-HCl buffer (pH 3–4), potassium phosphate buffer (pH4–8), Tris-HCl buffer (pH8–10) and glycine-HCl buffer (pH10–12). (B) The optimum temperature was measured at pH7.0 (100 mM potassium phosphate buffer) using vanillin as the substrate.

measure the activity of purified $VDH_{ATCC13032}$. $VDH_{ATCC13032}$ showed catalytic activity toward a broad range of tested substrates (Table S1), including vanillin, 3,4-dihydroxybenzaldehyde, 3-hydroxybenzaldehyde, *p*-hydroxybenzaldehyde, *p*-nitrobenzaldehyde, terephthalaldehyde and 2,4-dichlorobenzaldehyde; and $VDH_{ATCC13032}$ showed lower activities (less than 50% of that toward vanillin) toward *o*-phthaldialdehyde, cinnamaldehyde, syringaldehyde, benzaldehyde and benzenepropanal. However, phenylacetaldehyde, formaldehyde and aldehyde were not oxidized at detectable rates (rates lower than 5% of the enzyme activity with vanillin).

The catalytic efficiency of $VDH_{ATCC13032}$ toward vanillin, *p*-hydroyxlbenzaldehyde and 3,4-dihydroxybenzaldehyde was further tested by kinetics analysis (Table S2). The experimental results revealed that VDH had a higher affinity toward vanillin than to the other two substrates, and NAD^+ was a required cofactor for this reaction, with the same level of activity as replaced with $NADP^+$ (Table S3). This suggested that the enzyme could utilize both NAD^+ and $NADP^+$ as cofactors and show no obvious difference to them.

The catalytic activity of $VDH_{ATCC13032}$ was further confirmed by LC-MS analysis using the selected substrates. Purified $VDH_{ATCC13032}$ enabled the conversion of vanillin to vanillate (as shown in Figure 5). The HPLC results indicated that the production of vanillate in the presence of NAD^+ and $VDH_{ATCC13032}$ was coupled with the decrease of the vanillin concentration (Fig. 5A). The production of vanillate was also validated by MS analysis (Data not shown). Purified $VDH_{ATCC13032}$ also considerably converted 3,4-dihydroxybenzaldehyde to 3,4-dihydroxybenzoic acid (Fig. 5B).

Site-directed mutagenesis analysis of $VDH_{ATCC13032}$. Based on sequence alignment, E258 and C292 were identified as the candidate conserved catalytic residues whereas N157, K180 and E199 were identified as the candidate cofactor interactive sites in $VDH_{ATCC13032}$, and these residues were demonstrated to be essential for VDH from the hyperthermophilic archaeon *Sulfolobus tokodaii*[15] and *Pseudomonas aeruginosa*[16]. To investigate whether these five residues are also important for the $VDH_{ATCC13032}$ catalytic activity, $VDH_{ATCC13032}$ variants were constructed followed by *in vitro* catalytic assay using vanillin as the substrate in the presence of $NAD(P)^+$. As a result, in the presence of NAD^+, all the five variants showed activities of less than 50% of the wild type toward vanillin (Table S4). Interestingly, in the presence of $NADP^+$, the activities of N157A, K180A and C292A decreased to as low as 10% of the wild type enzyme; but for E199A, the catalytic activity still kept at 78% of the wild type enzyme (Table S4). In addition, while other variants showed more than six times higher Km values than the wild type toward $NADP^+$, the E199A variant showed significantly lower K_m (Table S5). Moreover, all the mutations showed decreased affinity to NAD^+ (Table S5). Thus, it could be speculated that E199 have less influence on binding $NADP^+$, compared with the other residues; however, all these residues play key roles in binding NAD^+. Furthermore, mutation of any of the five residues resulted in increased K_m values and decreased k_{cat} values toward vanillin (Table S6). Compared with the wild type enzyme, the deficient mutant of C292A, K180A and E258A had very lower affinities to vanillin (the K_m values was 4–9 times higher and the k_{cat}/K_m was 10–23 times lower, compared with the wild type enzyme). These results indicate that these residues also played important roles in the $VDH_{ATCC13032}$ to the affinity of substrate (e.g. vanillin).

Discussion

The *β*-ketoadipate pathway is the major catabolic route for lignin-derived aromatic compounds in soil bacteria[17–19]. In the present study, we cloned, expressed and functional characterized a *vdh* gene from *C. glutamicum*, which channeled a variety of lignin-derived aromatic compounds to the protocatechuate branch of *β*-ketoadipate pathway for further degradation. Based on the genome sequence of *C. glutamicum* ATCC13032[5,20], one putative aldehyde dehydrogenase gene, $vdh_{ATCC13032}$, was identified. But this gene does not show a remarkably high level of homology to those with verified vanillin dehydrogenase activity (Fig. 1). Our study suggests that $VDH_{ATCC13032}$ is probably a unique aldehyde dehydrogenase with special catalytic roles, as discussed in the following.

The conclusion that $VDH_{ATCC13032}$ is a vanillin dehydrogenase is based on at least three lines of independent evidence. First, analysis of a *vdh* deletion mutant revealed a delayed growth when 3, 4-dihydroxy benzaldehyde, 3-hydroxy benzaldehyde, vanillin, or ferulic acid was present as the sole carbon source, suggesting an important role of $vdh_{ATCC13032}$ in assimilation of these compounds. It is known that caffeic acid is not a direct target of VDH. However, when grown in the presence of caffeic acid, the *vdh* deletion mutant showed a delayed growth as well, supporting the idea that *vdh* is at the central pathway for catabolism of aromatic compounds. The growth defects of the mutant strain were complemented by expressing wild type *vdh* (Fig. 2). Thus the resulting phenotype was not due to the polar effects caused by deletion of the *vdh* gene. The delayed growth observed with the deletion mutant grown on the different substrates may indicate

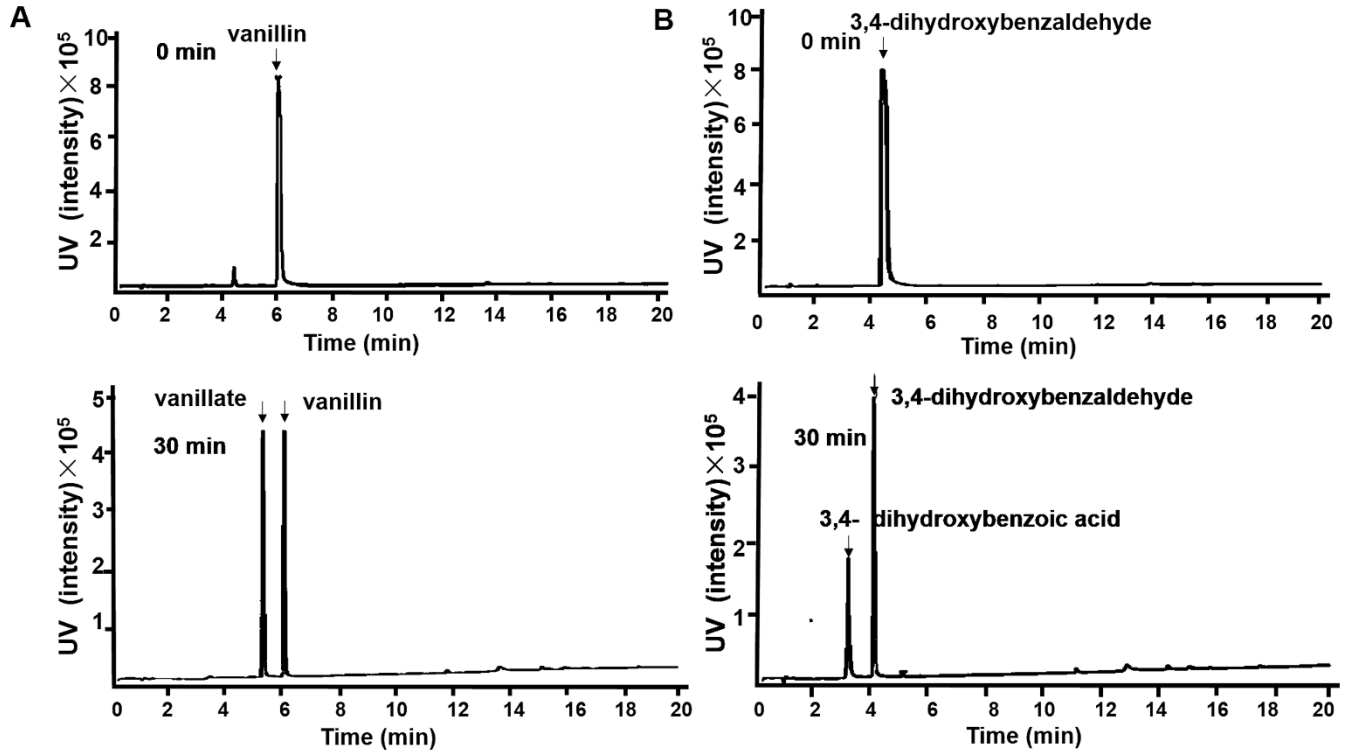

Figure 5 | Biotransformation of vanillin (A) and 3,4-dihydroxybenzaldehyde (B) with purified $VDH_{ATCC13032}$.

minor alternative pathways for catabolism of aromatic compounds. This is consistent with the *Amycolatopsis sp*. strain ATCC 39116, in which VDH also plays a significant role in the course of vanillin degradation, but the biotransformation from vanillin to vanillate were still observed when *vdh* gene was knocked out[21].

HPLC-MS was performed to examine the biotransformation products of $VDH_{ATCC13032}$ in the presence of vanillin or 3,4-dihydroxybenzaldehyde. As expected, vanillin and 3,4-dihydroxybenzaldehyde were transformed to vanillate and 3,4-dihydroxybenzoic acid, respectively, confirming the activity of $VDH_{ATCC13032}$. Relatively high catalytic activity of purified $VDH_{ATCC13032}$ was observed with *p*-hydroxylbenzaldehyde and vanillin, consistent with the fact that *vdh* gene is at the downstream of ferulate and *p*-coumarate metabolism pathway. Also, $VDH_{ATCC13032}$ was heterologously expressed and its Mr was estimated by SDS-PAGE (Fig. 3A). Interestingly, the native molecular mass determined by gel filtration showed that VDH from *C. glutamicum* existed in the form of tetramers, trimers and dimers (Fig. 3B and C). This is consistent with previous reports that VDHs from *Micrococcus* sp. TA1 and *Burkholderia cepacia* TM1 exist as tetramers and dimers, respectively[22]. The enzyme displayed the highest activity at 30°C, in accordance with the physiological temperature of *C. glutamicum* and the results of *in vitro* expression assay. VDH from most of the studied species showed specificity against vanillin and benzaldehyde compounds. While purified VDH from *C. glutamicum* ATCC13032 showed catalytic activity toward a relatively broad range of tested substrates (Table S1), oxidation rate for phenylacetaldehyde, formaldehyde and aldehyde were not detected. The observed substrate specificity is consistent with the substrate specificity observed with vanillin dehydrogenases from *S. paucimobilis* SYK-6[14] and *P. fluorescens*[9]. While most VDHs identified so far tend to use NAD^+ as a sole cofactor, $VDH_{ATCC13032}$ could utilize both NAD^+ and $NADP^+$, which has been observed with the VDH from *P. fluorescens* in a previous study[9]. Taken together, these results have revealed the important roles of VDH in *C. glutamicum* ATCC13032, whereas substrate specificity may vary from one species to another.

Extensive works have been done to examine the active amino acid residues in the ALDH enzymes, and the examined residues have been well documented[15,16,23]. Sequence alignment revealed conserved sequences in $VDH_{ATCC13032}$ with relatively high amino acid similarity with the active residues identified in ALDH and *Pa*BADH. One strictly conserved residue is Cys-292 in $VDH_{ATCC13032}$, which has been demonstrated to be responsible for the dehydrogenase as well as esterase activities of aldehyde dehydrogenase[16,24]. In *P. aeruginosa*, the *Pa*BADH catalytic cysteine (C286, corresponding to C292 in $VDH_{ATCC13032}$) is oxidized to sulfenic acid or forms a mixed disulfide with 2-mercaptoethanol[19]. The second active residue identified in $VDH_{ATCC13032}$ was Glu-258, which is in the vicinity of the catalytic cysteine, corresponding to E268 in ALDH2, E252 in PaBADH and E258 in VDH. This conserved residue probably functions as a general base in ALDH catalysis[25]. Lys-180 is another conserved residue in $VDH_{ATCC13032}$ and may have functions similar to that of ALDH (K78) and *Pa*BADH (K162)[16,23]. Glu-199 in the $VDH_{ATCC13032}$ may also be an conserved residue that would produce a steric clash with the 2′-phosphate of $NAD(P)^+$, resulting in a low affinity of ALDH2 for $NAD(P)^+$[16]. Therefore we speculated that these five conserved sites may be important for the catalytic activity of $VDH_{ATCC13032}$, and they were subjected to further characterization. Mutations of these residues decreased catalytic activities by more than 50% compared with wild type when NAD^+ was used as a cofactor. However, when $NADP^+$ was used as a cofactor, mutations of N157A, E258A and C292A caused 90% reduction of catalytic activities compared with wild type, while E199A mutation only reduced the activity by 12%. This indicates that Glu-199 may have less influence on $NADP^+$ binding compared with the other tested residues, whereas all these residues play roles in NAD^+ binding. Consistently, Glu-199 showed no effect on the affinity of $VDH_{ATCC13032}$ to $NADP^+$, but affected the affinity of $VDH_{ATCC13032}$ for the substrates such as vanillin. Taken together, the examined residues play critical roles in VDH catalysis, but their mechanisms may be different.

Lignocellulosic hydrolysates for biofuel production usually contain not only fermentable sugars but also non-fermentable growth inhibitors, including furan, weak acids, and various lignin-derived aromatic compounds (such as vanillin, ferulic acid, *p*-coumaric acid, 4-hydroxybenzoic acid, vanillic acid, etc.), which inhibit microbial

fermentation to the desired products[26,27]. *C. glutamicum* could be applied to both detoxify and assimilate lignin-derived aromatic inhibitors as an alternative source to sugars for carbon and energy. The functional characterization of $VDH_{ATCC13032}$ contributes not only to a systematical understanding of aromatic compound assimilation, but also to develop *C. glutamicum* as an efficient strain to convert lignocellulose to bioproducts, such as biofuels.

Methods

Bacterial strains, plasmids, and culture conditions. All bacterial strains and plasmids used in this study are listed in Table S7. *Escherichia coli* was cultivated at 37°C in Luria-Bertani (LB) medium[28]. *C. glutamicum* strains were routinely grown at 30°C in LB or in mineral salts medium (MM), which was adjusted to pH 8.4 and supplemented with yeast extract (0.05 g L^{-1})[4]. For generation of mutants and maintenance of *C. glutamicum*, BHIS (brain heart broth with 0.5 M sorbitol) medium was used[2]. *C. glutamicum* RES167, a restriction-deficient strain derived from *C. glutamicum* ATCC 13032 was the parent of all derivatives used in this study. Aromatic compounds were added to the MM medium at suitable final concentrations. Cell growth was monitored photometrically at 600 nm[12,29]. Kanamycin, chloramphenicol were added at final concentrations of 20 and 10 μg ml^{-1}, respectively for both *E. coli* and *C. glutamicum*, and ampicillin of 100 μg ml^{-1} for *E. coli*, whereas nalidixic acid of 40 μg ml^{-1} for *C. glutamicum*.

Gene prediction in the *C. glutamicum* genome. Translated BLAST search (blastx) from the National Center for Biotechnology Information (NCBI) was used to identify genes involved in vanillin catabolism in *C. glutamicum* ATCC13032 (Accession no. NC 003450). Through the BLAST analyses, homologues of the putative genes encoding vanillin dehydrogenase were identified. The phylogenetic tree including $vdh_{ATCC13032}$ and *vdh* genes from other bacteria was constructed by ClustalX 1.83 and Molecular Evolutionary Genetics Analysis (MEGA), and the calculation were performed using the neighbor-joining method[30].

DNA manipulations and plasmid construction. Genomic DNA of *C. glutamicum* was isolated according to the method described by Tauch *et al.*[31]. Plasmids were isolated with plasmid DNA miniprep spin columns (TIANGEN, Beijing, China), and DNA fragments were purified from agarose gels by EasyPure Quick Gel Extraction Kit (TransGen Biotech, Beijing, China). *C. glutamicum* was transformed by electroporation according to the method of Tauch *et al.*[31]. Competent cells of *E. coli* were prepared and transformed using the $CaCl_2$ procedure[29]. Target DNA fragments were PCR amplified and digested by standard methods. All plasmids were constructed based on pK18*mobsacB*, pXMJ19, or pET28a. Primers used are listed in Table S8. To construct the plasmid for *ncgl2578* knock out, the upstream and downstream DNA fragments were amplified using primer pairs ncgl2578upFBamHI/ncgl2578upR and ncgl2578dwF/ncgl2578dwRHindIII, respectively. The upstream and downstream PCR fragments were linked together by overlap PCR and then inserted into pK18*mobsacB* to generate pK18*mobsac-Δncgl2578* through restriction enzyme digestion. For complementation, plasmid pXMJ19-*ncgl2578* was created by insertion of the PCR-amplified ORF into pXMJ19. Plasmid for expression of the target gene in *E. coli* was constructed from PCR-amplified gene and pET28a. All the constructed plasmids were confirmed by DNA sequencing.

Construction of the *vdh* mutant and complementary strain in *C. glutamicum*. To construct the *vdh* mutant, the plasmid pK18*mobsacBΔncgl2578* was transformed into *C. glutamicum* RES167 by electroporation, and chromosomal integration was selected by plating on LB agar plates supplemented with kanamycin. The *Δncgl2578* deletion mutant was subsequently screened on LB agar plates containing 10% sucrose and confirmed by PCR and sequencing as previously described[20]. For complementation, pXMJ19-*ncgl2578* was transformed into the mutant strain and *vdh* gene expressed in *C. glutamicum* was induced by addition of 0.5 mM isopropyl-D-thiogalactopyranoside (IPTG) to the culture broth.

Expression and purification of recombinant VDH in *E. coli*. To express the His_6-VDH protein, recombinant plasmid pET28a-*ncgl2578* was electroporated into *E. coli* BL21 (DE3). When the growth of recombinant *E. coli* reached OD_{600} = 0.4, the expression of recombinant protein was initiated by addition of 0.5 mM IPTG, and the culture was then shaked overnight at 22°C[11]. Cells were harvested by centrifugation at 10,000 g for 10 min at 4°C, washed twice with ice-cold phosphate-buffered saline (PBS). Harvested cells were disrupted by sonication and purified with the His·Bind Ni-NTA resin (Novagen, WI, USA) following the manufacturer's instructions. Purified recombinant protein was dialyzed against PBS overnight at 4°C and stored at −80°C until use. Protein concentrations were determined using the Bradford assay according to the manufacturer's instructions (Bio-Rad, Hercules, CA) with bovine serum albumin as the standard.

SDS-PAGE and determination of molecular mass of the purified enzyme. SDS-PAGE was conducted with 5% stacking gels and 10% resolving gel and run in a Mini-PROTEIN II Electrophoresis Cell (Bio-Rad) according to the manufacturer's instructions. After electrophoresis, the protein bands were visualized by Coomassie brilliant blue staining. Apparent molecular mass was estimated according to the relative mobility of Blue Plus II protein markers, with molecular masses ranging from 14 to 120 kDa. The native molecular mass of the VDH was estimated by gel filtration chromatography on a Superdex 200 10/300 GL column (1.0 cm × 30 − 31 cm) (Amersham BioSciences) eluted at a flow rate of 0.25 ml min^{-1} with 100 mM potassium phosphate buffer containing 150 mM NaCl (pH 7.2). Molecular weight standards used are: hyroglobulin (bovine) (670 kDa), γ-globulin (bovine) (158 kDa), Ovalbumin (chicken) (44 kDa), Myoglobin (horse) (17 kDa) and Vitamin B12 (1.35 kDa). To characterize the molecular configuration of the purified VDH, we employed PAGE under nondenaturing conditions. Gels consisted of a separating gel (15% acrylamide) and a stacking gel (5% acrylamide) and the loading buffer was also under nondenaturing condition, which contained 0.5 M Tris-HCl buffer (pH 6.8), 0.1% bromophenol blue and 10% glycerin. The Sample containing 40 μg protein was loaded, and then electrophoresis was carried out at 4°C in Tris-glycine buffer (25 mM Tris-base, 250 mM Glycine). Apparent molecular mass was estimated according to the relative mobility of protein markers Protein Rule IV (TransGen Biotech, Beijing, China), with molecular masses ranging from 30 to 200 kDa.

Enzyme assays. The VDH enzyme assay was performed based on described methods[32–34] in 100 mM potassium phosphate buffer (pH 7.0). The activity of vanillin dehydrogenase was monitored spectrophotometrically by measuring the rate of decrease in absorption at 340 nm due to oxidation of NAD(P)H and was calculated with an extinction coefficient of 6,220 M^{-1} cm^{-1}. The reaction mixture (1 ml) contained substrate (1 mM), $NAD(P)^+$ (0.5 mM) and an appropriate amount of enzyme in potassium phosphate buffer (100 mM, pH 7.0). The optimal pH was determined in various pHs of 100 mM buffer as follows: glycine-HCl buffer (pH 3–4), potassium phosphate buffer (pH4–8), Tris-HCl buffer (pH8–10) and glycine-HCl buffer (pH10–12). One unit of enzyme activity was defined as the amount of enzyme producing 1 mmol NAD(P)H min^{-1} as previously described[15,33]. Specific activities were given as unit mg^{-1} of protein[35]. Protein concentrations were determined using the Bradford assay with bovine serum albumin as standard.

Biotransformation of aromatic compounds with recombinant VDH. To further analyze the biotransformation of aromatic compounds, the purified VDH from *C. glutamicum* strains was added to the reaction mixture (1 ml) containing substrate (1 mM) and NAD^+ (0.5 mM) in potassium phosphate buffer (100 mM, pH 7.0). The reaction was performed at room temperature for 30 min, and a parallel mixture without VDH enzyme was used as a negative control. The products were analyzed by high-performance liquid chromatography-mass spectrometry (HPLC-MS) as previously described[36,37]. To confirm the vanillate and 3,4-dihydroxybenzoic acid as products in the two test reactions, standard compound were used as controls, and the molecular weight of the products were verified based on MS analysis. The wavelength for UV detection was set at 275 nm.

Site-directed mutagenesis. To identify the potential active residues in the VDH from *C. glutamicum* ATCC13032, genes from ALDH (aldehyde dehydrogenase) family with known active sites, such as ALDH2 and *Pa*BADH (*Pseudomonas aeruginsa* betaine aldehyde) were used as references for alignment analysis. The alignment suggested that the five known residues were also present in the $VDH_{ATCC13032}$. Subsequently overlap PCR was performed to construct site-directed mutants of $VDH_{ATCC13032}$ protein using five pairs of primers according to the standard PCR-based mutagenesis. In detail, the following mutants were designed: N157A, K180A, E199A, E258A and C292A. Activities and kinetics parameters of all the mutants were determined with the experimental procedures of wild type enzyme described above[15].

1. Lee, J. *et al.* Succinate production from CO2-grown microalgal biomass as carbon source using engineered *Corynebacterium glutamicum* through consolidated bioprocessing. *Sci Rep* **4**, 5819 (2014).
2. Shen, X. H., Jiang, C. Y., Huang, Y., Liu, Z. P. & Liu, S. J. Functional identification of novel genes involved in the glutathione-independent gentisate pathway in *Corynebacterium glutamicum*. *Appl Environ Microbiol* **71**, 3442–3452 (2005).
3. Shen, X. H., Zhou, N. Y. & Liu, S. J. Degradation and assimilation of aromatic compounds by *Corynebacterium glutamicum*: another potential for applications for this bacterium? *Appl Microbiol Biotechnol* **95**, 77–89 (2012).
4. Huang, Y. *et al.* Genetic characterization of the resorcinol catabolic pathway in *Corynebacterium glutamicum*. *Appl Environ Microbiol* **72**, 7238–7245 (2006).
5. Ikeda, M. & Nakagawa, S. The *Corynebacterium glutamicum* genome: features and impacts on biotechnological processes. *Appl Microbiol Biotechnol* **62**, 99–109 (2003).
6. Merkens, H. *et al.* Vanillate metabolism in *Corynebacterium glutamicum*. *Curr Microbiol* **51**, 59–65 (2005).
7. Brinkrolf, K., Brune, I. & Tauch, A. Transcriptional regulation of catabolic pathways for aromatic compounds in *Corynebacterium glutamicum*. *Genet Mol Res* **5**, 773–789 (2006).
8. Havkin-Frenkel, D. & Belanger, F. Biotechnology of Vanillin: Vanillin from Microbial Sources. *Handbook of Vanilla Science and Technology* **301**, (eds Wily-Blackwell) (ISBC press. 2010).
9. Di Gioia, D. *et al.* Metabolic engineering of *Pseudomonas fluorescens* for the production of vanillin from ferulic acid. *J Biotechnol* **156**, 309–316 (2010).
10. Plaggenborg, R., Overhage, J., Steinbüchel, A. & Priefert, H. Functional analyses of genes involved in the metabolism of ferulic acid in *Pseudomonas putida* KT2440. *Appl Microbiol Biotechno* **61**, 528–535 (2003).

11. Shaw, J. P. & Harayama, S. Purification and characterisation of TOL plamids-encoded benzyl alcohol dehydrogenase and benzaldehyde dehydrogenase of *Pseudomonas putida*. *Eur J Biochem* **191**, 705–714 (1990).
12. Overhage, J., Priefert, H., Rabenhorst, J. & Steinbüchel, A. Biotransformation of eugenol to vanillin by a mutant of *Pseudomonas* sp. strain HR199 constructed by disruption of the vanillin dehydrogenase gene. *Appl Microbiol Biotechnol* **52**, 820–828 (1999).
13. Masai, E. *et al*. Cloning and Characterization of the Ferulic Acid Catabolic Genes of *Sphingomonas paucimobilis* SYK-6. *Appl Environ Microbiol* **68**, 4416–4424 (2002).
14. Masai, E. *et al*. Characterization of ligV Essential for Catabolism of Vanillin by *Sphingomonas paucimobilis* SYK-6. *Biosci Biotechnol Biochem* **71**, 2487–2492 (2007).
15. Liu, T., Hao, L., Wang, R. & Liu, B. Molecular characterization of a thermostable aldehyde dehydrogenase (ALDH) from the hyperthermophilic archaeon *Sulfolobus tokodaii* strain 7. *Extremophiles* **17**, 181–190 (2013).
16. González-Segura, L., Rudiño-Piñera, E., Muñoz-Clares, R. A. & Horjales, E. The crystal structure of a ternary complex of betaine aldehyde dehydrogenase from *Pseudomonas aeruginosa* provides new insight into the reaction mechanism and shows a novel binding mode of the 2'-phosphate of $NADP^+$ and a novel cation binding site. *J Mol Biol* **385**, 542–557 (2009).
17. Davis, J. R. & Sello, J. K. Regulation of genes in *Streptomyces* bacteria required for catabolism of lignin-derived aromatic compounds. *Appl Microbiol Biotechnol* **86**, 921–929 (2010).
18. Harwood, C. S. & Parales, R. The beta-ketoadipate pathway and the biology of self-identity. *Annu Rev Microbiol* **50**, 553–590 (1996).
19. Shen, X. H. & Liu, S. J. Key enzymes of the protocatechuate branch of the *β*-ketoadipate pathway for aromatic degradation in *Corynebacterium glutamicum*. *Science in China Series C* **48**, 241 (2005).
20. Shen, X. H., Huang, Y. & Liu, S. J. Genomic analysis and identification of catabolic pathways for aromatic compounds in *Corynebacterium glutamicum*. *Microbes and Environents* **20**, 160–167 (2005).
21. Fleige, C., Hansen, G., Kroll, J. & Steinbüchel, A. nvestigation of the *Amycolatopsis sp*. strain ATCC 39116 vanillin dehydrogenase and its impact on the biotechnical production of vanillin. *Appl Environ Microbiol* **79**, 81–90 (2013).
22. Mitsui, R., Hirota, M., Tsuno, T. & Tanaka, M. Purification and characterization of vanillin dehydrogenases from alkaliphile *Micrococcus sp.* TA1 and neutrophile *Burkholderia cepacia* TM1. *FEMS Microbiol Lett* **303**, 41–47 (2010).
23. Díaz-Sánchez, A. G. *et al*. Novel NADPH-cysteine covalent adduct found in the active site of an aldehyde dehydrogenase. *Biochem J* **439**, 443–452 (2011).
24. Priefert, H., Rabenhorst, J. & Steinbüchel, A. Molecular character of *Pseudomonas* sp. Strain HR199 involved in bioconversion of vanillin to protocachuate. *J Bacteriol* **179**, 2595–2607 (1997).
25. Wang, X. P. & Weiner, H. Involvement of glutamate-268 in the active-site of human liver mitochondrial (class-2) aldehyde dehydrogenase as probed by site-directed mutagenesis. *Biochemistry* **34**, 237–243 (1995).
26. Almeida, J. R. *et al*. NADH- vs NADPH-coupled reduction of 5-hydroxymethyl furfural (HMF) and its implications on product distribution in *Saccharomyces cerevisiae*. *Appl Microbiol Biotechnol* **78**, 939–945 (2008).
27. Klinke, H. B., Thomsen, A. B. & Ahring, B. K. Inhibition of ethanol-producing yeast and bacteria by degradation products produced during pre-treatment of biomass. *Appl Microbiol Biotechnol* **66**, 10–26 (2004).
28. Achterholt, S., Priefert, H. & Steinbüchel, A. Identification of *Amycolatopsis* sp. strain HR167 genes, involved in the bioconversion of ferulic acid to vanillin. *Appl Microbiol Biotechnol* **54**, 799–807 (2000).
29. Overhage, J., Priefert, H. & Steinbüchel, A. Biochemical and genetic analyses of ferulic acid catabolism in *Pseudomonas* sp. strain HR199. *Appl Environ Microbiol* **65**, 4837–4847 (1999).
30. Saitou, N. & Nei, M. The neighbor-joining method. A new method for reconstructing phylogenetic trees. *Mol Biol Evol* **4**, 406–425 (1987).
31. Tauch, A., Kassing, F., Kalinowski, J. & Pühler, A. The *Corynebacterium xerosis* composite transposon Tn5432 consists of two identical insertion sequences, designated IS1249, flanking the erythromycin resistance geneermCX. *Plasmid* **34**, 119–131 (1995).
32. Baré, G., Swiatkowski, T., Moukil, A., Gerday, C. & Thonart, P. Purification and characterization of a microbial dehydrogenase: a vanillin:$NAD(P)^+$ oxidoreductase. *Appl Biochem Biotechnol* **98**, 415–428 (2002).
33. Peng, X. *et al*. Characterization of *Sphingomonas* aldehyde dehydrogenase catalyzing the conversion of various aromatic aldehydes to their carboxylic acids. *Appl Microbiol Biotechnol* **69**, 141–150 (2005).
34. Yang, W. *et al*. Characterization of two Streptomyces enzymes that convert ferulic acid to vanillin. *PloS one* **8**, e67339 (2013).
35. MacKintosh, R. W. & Fewson, C. A. Benzyl alcohol dehydrogenase and benzaldehyde dehydrogenase II from *Acinetobacter calcoaceticus*. Purification and preliminary characterization. *Biochem J* **250**, 743–751 (1988).
36. Kaur, B., Chakraborty, D. & Kumar, B. Phenolic biotransformations during conversion of ferulic acid to vanillin by *Lactic acid* bacteria. *Biomed Res Int* **2013**, 590359 (2013).
37. Saa, L., Jaureguibeitia, A., Largo, E., Llama, M. J. & Serra, J. L. Cloning, purification and characterization of two components of phenol hydroxylase from *Rhodococcus erythropolis* UPV-1. *Appl Microbiol Biotechnol* **86**, 201–211 (2010).
38. Plaggenborg, R. *et al*. Potential of *Rhodococcus* strains for biotechnological vanillin production from ferulic acid and eugenol. *Appl Microbiol Biotechnol* **72**, 745–755 (2006).
39. Sekine, M. *et al*. Sequence analysis of three plasmids harboured in *Rhodococcus erythropolis* strain PR4. *Environ Microbiol* **8**, 334–346 (2006).
40. Chen, H. P. *et al*. Vanillin catabolism in *Rhodococcus jostii* RHA1. *Appl Environ Microbiol* **78**, 586–588 (2012).
41. Shrivastava, R., Basu, A. & Phale, P. S. Purification and characterization of benzyl alcohol- and benzaldehyde- dehydrogenase from *Pseudomonas putida* CSV86. *Arch Microbiol* **193**, 553–563 (2011).
42. Venturi, V., Zennaro, F., Degrassi, G., Okeke, B. C. & Bruschi, C. V. Genetics of ferulic acid bioconversion to protocatechuic acid in plantgrowth-promoting *Pseudomonas putida* WCS358. *Microbiology* **144**, 965–973 (1998).
43. Nelson, K. E. *et al*. Complete genome sequence and comparative analysis of the metabolically versatile *Pseudomonas putida* KT2440. *Environ Microbiol* **4**, 799–808 (2002).
44. Gasson, M. J. *et al*. Metabolism of Ferulic Acid to Vanillin A bacterial gene of the enoyl-SCoA hydratase/isomerase superfamily encodes an enzyme for the hydration and cleavage of a hydroxycinnamic acid SCoA thioester. *J Biol Chem* **273**, 4163–4170 (1998).

Acknowledgments

This work was supported by the National High Technology Research and Development Program of China (863 program, grant 2013AA102802), National Natural Science Foundation of China (31270078), Key Science and Technology R&D Program of Shaanxi Province, China (2014K02-12-01) and Fundamental Research Funds for the Central Universities, Northwest A&F University (Z111021006).

Author contributions

W.D., W.Z., S.C. and X.S. wrote the main manuscript. W.D., M.S., W.Z., Y.Z., C.C., L.Z., Z.L. and X.S. designed and performed the experiments. W.D., M.S., W.Z., S.C. and X.S. analyzed the data. W.D. and C.C. prepared samples. All authors discussed and reviewed the manuscript.

Additional information

Supplementary information accompanies this paper at http://www.nature.com/scientificreports

Competing financial interests: The authors declare no competing financial interests.

How to cite this article: Ding, W. *et al*. Functional characterization of a vanillin dehydrogenase in *Corynebacterium glutamicum*. *Sci. Rep.* **5**, 8044; DOI:10.1038/srep08044 (2015).